Journal of the Brazilian Society of Mechanical Sciences and Engineering (2023) 45:530
https://doi.org/10.1007/s40430-023-04456-8

TECHNICAL PAPER

Environmental drawbacks of lightweight design algorithms in material extrusion additive manufacturing: a case study

Mattia Mele[1] · Gregorio Pisaneschi[1] · Michele Ciotti[1] · Giampaolo Campana[1] · Andrea Zucchelli[1] · Maurizio Fiorini[2]

Received: 11 January 2023 / Accepted: 28 August 2023

Abstract

Lightweight design is often assumed to be the leading strategy to improve the sustainability of parts produced by additive manufacturing. The present study confutes such an assumption by a cradle-to-gate life cycle assessment of different lightweight strategies applied to a specific case study in the medical field. In particular, a patient-specific finger splint made of polyamide is redesigned by means of generative design, topology optimization and lattice structures. The analysis investigates two markedly different deposition processes, namely Arburg plastic freeforming and fused filament fabrication. The former is carried out on an industrial-grade machine, while a desktop printer is used for the latter. This allows for observing the impact of the redesign in two quite distinct scenarios. Findings demonstrate that, since environmental impacts are mainly driven by building time, the adoption of automated design algorithms can be detrimental to the sustainability of the process. On the other hand, relevant benefits on environmental impacts were achieved by reducing the infill percentage of parts. The results of this work highlight the most relevant aspects which must be considered to limit environmental impacts when designing parts for deposition-based additive manufacturing. This information can be used by designers to drive weight reduction towards sustainability.

Keywords Additive manufacturing · Arburg plastic freeforming · Fused filament fabrication · Sustainability

1 Introduction

Additive Manufacturing (AM) is becoming increasingly important in modern industry [1]. Initially adopted principally for prototyping, these technologies are nowadays used for the production of final parts in several industrial fields [2]. The market for AM is expected to increase exponentially in the near future fostered by technological innovations and new application fields [3, 4].

The tremendous expansion of AM determined a surge of interest in the sustainability of these technologies. Specifically, a number of studies have been carried out to assess the Environmental Impact (EI)s of these processes [5–7]. The studies in this field are mainly carried out by means of Life Cycle Assessment (LCA) in order to quantify the impact of each aspect of the production on EIs [8, 9]. Findings in this field point out three main sources of EI, namely equipment, energy and material consumption [10, 11]. The latter aspect received great attention since it allows for exploiting the potential of these technologies. In fact, AM permits the manufacturing of complex geometries which cannot be fabricated by traditional processes [12]. This peculiarity opens

Technical Editor: Zilda de Castro Silveira.

✉ Mattia Mele
mattia.mele@unibo.it

Gregorio Pisaneschi
gregorio.pisaneschi@unibo.it

Michele Ciotti
michele.ciotti4@unibo.it

Giampaolo Campana
giampaolo.campana@unibo.it

Andrea Zucchelli
a.zucchelli@unibo.it

Maurizio Fiorini
maurizio.fiorini@unibo.it

[1] Department of Industrial Engineering (DIN), University of Bologna, Viale del Risorgimento 2, 40136 Bologna, Italy

[2] Department of Civil, Chemical, Environmental and Materials Engineering (DICAM), University of Bologna, Viale del Risorgimento 2, 40136 Bologna, Italy

Published online: 21 September 2023

the door to new design solutions minimising the amount of material comprising the product. Such a trend is strongly supported by Computer Aided Design (CAD) and Computer Aided Engineering (CAE) tools for the automated Lightweight Design (LWD) of parts based on user-defined criteria [13–15].

Generative Design (GD) is a quite recent approach to LWD based on the application of evolutionary Artificial Intelligence (AI) techniques to modelling. According to [16], GD can be defined as a designer-driven, parametrically constrained design exploration process, operating on top of history-based parametric CAD systems. The GD process starts from a user-defined model and iteratively modifies the design based on performance indicators defined by the user. Modifications must respect design constraints imposed by the user [17]. In recent years, this design method has been extensively applied to AM for the redesign of parts by reducing weight [18, 19].

Another widespread approach to LWD is based on the use of Lattice Structures (LS). These structures consist of elementary geometries that are replicated in the space to replace the original part volume [14]. LS can be arranged in the 3D space according to different schemes. Voronoi diagram is a popular solution which allows for easily achieving a non-uniform distribution of elements on complex geometries [20]. LS has been extensively used for the design of parts by AM processes due to their relatively low computational cost if compared to GD [21].

Several studies highlighted the reduction of EI during the product use phase achievable through LWD [6]. Such advantages are particularly relevant for applications to transportation, where the part weight is strictly connected to energy consumption [22]. The findings in these fields demonstrate that AM-enabled LWD can bring tremendous benefits to the sustainability of the final product during usage [23, 24]. Research in this field provides an in-depth insight into the possibilities offered by AM technologies in strategic fields. Nevertheless, these studies do not consider the role of LWD on the EI associated with the production phase. As a result, LWD is generally considered to play a positive role in determining the sustainability of parts by AM, which is assumed to provide *"complexity-for-free"* [25]. These studies highlight marvellous opportunities in the usage phase but fail to investigate the effects of LWD on the cradle-to-gate phase of the lifecycle. Nonetheless, previous research highlighted that this phase strongly affects the economic, social and environmental sustainability of AM [26, 27]. Specifically, the EI of the production is driven by material usage, energy consumption and waste volume [28–30]. These factors in turn change with the geometry and orientation of parts, which may thus strongly affect the overall process sustainability [31, 32]. Therefore, it is necessary to take the EIs of the production since the first phases of the design [33, 34]. Previous studies proposed dedicated approaches to part design in order to reduce material and energy consumption [35, 36]. Nonetheless, to date, no research investigated the role of existing LWD methods on EIs of AMed products. This is of great relevance since these methods are made available in commercial software and are most commonly adopted in real industrial scenarios.

The present study investigates the effects of LWD techniques on environmental impact in a case study. The main aim is to demonstrate that, for the case study, weight reduction is not sufficient to improve the sustainability of the product.

The analysis is carried out by comparing two radically different Material Extrusion (MEX) processes, namely Arburg Plastic Freeforming (APF) and Fused Filament Fabrication (FFF). The former is carried out on industrial equipment, while a desktop machine is considered for the latter. This allows for observing the effects of the redesign in two profoundly different scenarios. It is worth remarking that the scope of this study is to compare different LWD strategies, while a comparison between the MEX processes is not possible due to their differences in terms of requirements and product quality [37].

The case study analysed in this paper is a Patient-Specific Finger Splint (PSFS). This product has been chosen since the need for customisation makes it especially suitable for AM. Moreover, its shape and dimensions are suitable to both the MEX processes considered in this study, also if more than one product unit is manufactured. Since APF is widely used in the medical field, this machine can be found in hospital facilities [38]. Since the PSFS device is for external use, the parts processed by FFF are also compatible with the application.

The redesign of the PSFS is performed by means of different computer-based LWD algorithms, namely LS, GD and Topological Optimization (TO). Moreover, a non-complete infill strategy of the original design is included in the analysis. The different combinations between these LWD techniques and the MEX processes mentioned above are analysed by means of cradle-to-gate LCA to evaluate the variations of EI determined by the redesign.

2 Materials and methods

2.1 Part design

A PSFS has been designed for the scope of this study. The shape of the model is defined starting from two orthogonal pictures of the finger, as shown in Fig. 1.

In greater detail, four splines have been drawn on the profile of the finger. Then, a boundary blend function has

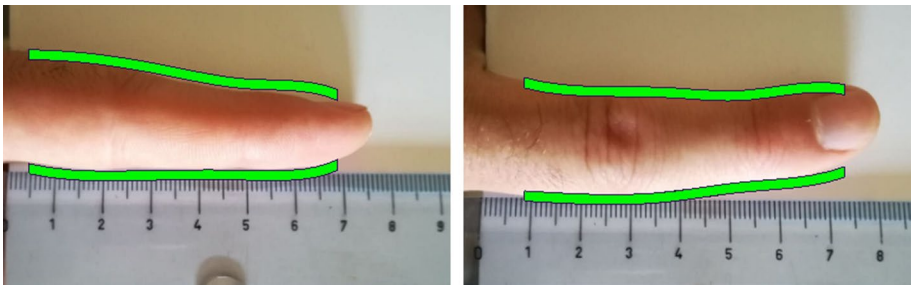

Fig. 1 Modelling of the finger splint (in green) starting from orthogonal pictures

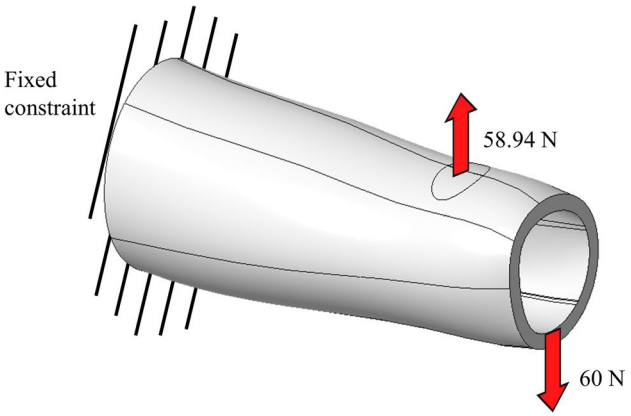

Fig. 2 Load conditions imposed for GD

been used to create a surface through these curves. Finally, the surface was thickened by 2 mm outwards to create a solid model. These operations were carried out using CAD software Creo Parametric by PTC©. The obtained part, which will be named Full Part Design (FPD) in the following, is used as a starting point for LWD.

Two automated LWD techniques are considered within the scope of this study, namely GD and LS.

GD has been performed using the dedicated module of PTC Creo Parametric 8. The loading conditions presented by [39] and shown in Fig. 2 have been used for calculation.

The PSFS is required to prevent flexion of the distal interphalangeal joint, which could impede the healing process [40]. According to the previous literature, the bottom face of the PSFS, i.e. the region at the base of the finger, is assumed to be fully constrained. The contraction of the finger is modelled by means of two forces with opposite directions. Specifically, a downward force is applied to the base of the distal phalange and an upward force is applied at the palm of the distal interphalangeal joint. According to the hypotheses by Emzain et al., the modules of these two forces are assumed to be equal to 60 N and 58.94 N, respectively [39]. Figure 2 depicts these loading conditions.

Specifically, the part is considered to be fully constrained at the bottom, i.e. at the base of the finger. The bending force is simulated by applying a load equal to 60 N to the opposite end and a resistant force with an opposite direction and module 58.94 N is applied at the palm of the distal phalanges joint [39]. The properties of Polyamide 6 (PA6) from the Granta database embedded in Creo are assumed. A target weight reduction equal to 50% is set. 512,373 elements with a maximum size of 0.257 mm are used for calculation. It is worth mentioning that, since the only objective of the optimization is weight reduction, GD returns a single design solution. When multiple objectives are defined, a set of pseudo-optimal alternatives is proposed by the software.

TO is carried out by means of the Ansys©simulation suite. The initial design space is assumed equal to the geometry of the FPD. The material properties, constraints and loads are equal to those used for GD and described above.

LS are designed by means of Creo Parametric. A Voronoi diagram with target cell size equal to 7 mm is used. The structure consists of beams with 2 mm diameters. Two solid annular regions of 2 mm height are defined at the top and bottom of the splint. The aim of these shapes is to prevent scratching of the finger while wearing and removing the splint.

All calculations have been run using an Intel® Xeon® E5-2620 v4 CPU @2.10GHz with 32 GB RAM.

2.2 Materials and processing conditions

The PSFS is designed to be made of PA6. Water solvable material, namely Polyvinyl Alcohol (PVA), is used to fabricate support structures.

The APF process is referred to an APF-2X 300K machine. The main processing parameters of PA6 and PVA on this machine are summarised in Table 1.

These parameters refer to Radilon S PA6 by Radici Group and Armat12 PVA by Arburg Gmbh, and were defined by means of a preliminary procedure for the characterisation of these materials [41].

All the job processing for calculating building time and material consumption has been carried out using the MiniMagics slicing software released by Arburg Gmbh ©.

The FFF is considered to be carried out on a Prusa i3 MK3S machine. Prusa Slicer software has been used for calculations. The processing parameters used are those provided by the software for Filatech PA and Primaselect

Table 1 Parameters used for APF printing

Parameter	Radilon S	Armat12
Extruding temperature (°C)	270	195
Build chamber temperature (°C)	110	
Number of perimeters	1	1
Perimeters deposition speed (mm/s)	15	20
Infill deposition speed (mm/s)	60	65
Infill direction (°)	± 45	± 45
Travelling speed (mm/s)	150	150
Layer height (mm)	0.2	
Drop aspect ratio	1.2	1.65

PVA+. The most relevant of these settings are summarised in Table 2.

2.3 Life cycle assessment

The analyses of EIs were carried out by adapting parametric LCA frameworks provided in the literature. Specifically, the LCA models presented by [37] and [42] are used for APF and FFF, respectively. Both these frameworks are based on the Ecoinvent dataset [43] and adopt the ReCiPe 2016 methodology [44] for Life Cycle Impact Assessment (LCIA). For the scope of the analysis, the machines are considered to be located in Bologna, Italy. The analyses are parametrised based on the material consumption and building time required for printing. Both these values can be calculated by means of slicing software.

The part and support material mentioned in Sect. 2.2 are used in place of those in the studies mentioned above. Specifically, the Ecoinvent dataset for the production of PA6 in the European region is used to model part material production. Since the Ecoinvent database does not include a dataset for the production of PVA, the one provided by the Product Environmental Footprints (PEF) of the European Commission has been used [45].

Table 2 Parameters used for FFF printing

Parameter	Filatech PA	Primaselect PVA+
Extruding temperature (°C)	275	195
Bed temperature (°C)	110	
Number of perimeters	2	2
External perimeters deposition speed (mm/s)	25	25
Internal perimeters deposition speed (mm/s)	45	45
Infill deposition speed (mm/s)	80	80
Infill direction (°)	± 45	± 45
Travelling speed (mm/s)	180	180
Layer height (mm)	0.2	
Line width (mm)	0.45	0.45

2.4 Design of experiment

To investigate the effects of design and part planning on EI, a full-factorial Design Of Experiment (DOE) is used. The first factor of the experiment considers the different designs, namely GD, TO, LS and FPD. Also, a solution in which the FPD is manufactured with a 50% infill is considered. This solution, named Full Part Design (50% infill) (FPD50), is included since a non-complete infill is an easy and widespread method to reduce the building time and material consumption in deposition processes.

The second factor considered in the DOE is the Part Build Orientation (PBO), i.e. the orientation of the part on the building plate. Previous literature has demonstrated that this aspect dramatically affects the energy and material consumption of AM. Within the scope of this study, three PBOs are considered. Specifically, the normal vector to the base plane of the PSFS is oriented at 0°, 45° and 90° to the *Z*-axis, as shown in Fig. 3.

The third and last factor of the DOE is the number of parts (n_p) on the printing tray. This aspect is particularly relevant to the production planning of AM businesses. The present study considers two scenarios. In the first, a single part is produced within the build job. In the second scenario, the building tray is filled with the maximum number of parts nestable in the given orientation. The nesting procedure is carried out by means of the slicing software mentioned above. It is worth mentioning that, since the case study deals with a custom device, the case in which numerous units of the same parts have to be produced is unlikely. Nonetheless, it is assumed that this configuration is representative of a more realistic situation in which a number of slightly different PSFSs must be produced simultaneously for various patients.

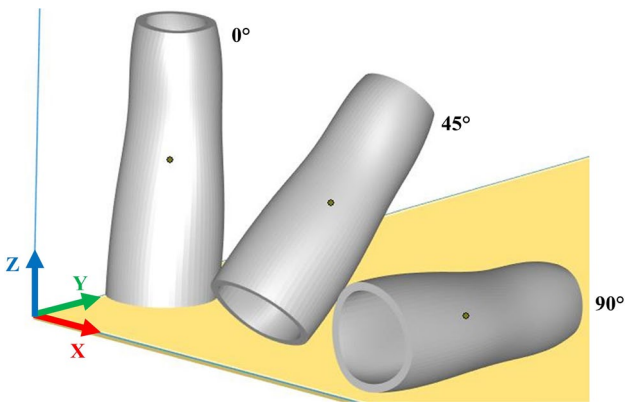

Fig. 3 Investigated PBOs

3 Results and discussion

3.1 Lightweight design

The geometry of the parts obtained by GD, TO and LS are shown, respectively, in Figure 4a–c.

Table 3 presents a summary of the information regarding solutions obtained through the use of LWD algorithms. The table reports the nominal volume and total surface area of each Computer-Aided Design (CAD) geometry, as well as the computational time required for different solutions. Additionally, the last two columns of Table 3 provide the maximum Von-Mises stress ($\sigma_{VM,max}$) and displacement (f_{max}) of each design. For GD and TO, $\sigma_{VM,max}$ and f_{max} are calculated during part generation, whereas for LS, a validation Finite Element Analysis (FEA) was conducted on the final geometry using PTC Creo.

As it can be noticed, GD is highly time-consuming if compared to TO. This is an expected result which can be explained by considering the iterative procedure adopted by GD and the structural analysis carried out at each step [21]. Moreover, LS is remarkably faster than the other two LWD techniques analysed, namely GD and TO, as it does not require a FEA of the part at each iteration. The final LS design comprises 7502 beams and 3803 nodes. The results presented in Table 4 indicate that the total surface area of this solution is more than twice that of GD and TO. Consequently, this leads to a higher number of contour lines during the printing process, in contrast to the other design solutions.

Table 3 Data of the parts generated via LWD

	Volume (mm^3)	Surface area (mm^2)	Computational time (s)	$\sigma_{VM,max}$ (MPa)	f_{max} (mm)
GD	4,421	6,179	10,806	11.35	0.64
LS	4,484	13,303	12	14.86	0.57
TO	4,814	5,846	467	8.1	0.47

3.2 Slicing

Tables 4 and 5 report the results of slicing for APF and FFF, respectively. Specifically, the building time (t_b), building time per part (t_{bp}), part mass(m_p) and support mass (m_s) are summarised.

By comparing Tables 4 and 5, it can be seen that APF requires significantly more time for processing. This result is expected since the droplet-by-droplet building strategy is slower than continuous deposition (see also Tables 1 and 2).

The building time per part t_{bp} is slightly higher when multiple parts are printed in the same job. This small difference is due to the rapid travel movements of the deposition head between parts. It is worth mentioning that this calculation does not consider the manual time required for part removal and job restarting, which is highly relevant in the case of single part printing.

By observing the support mass values (m_s), it can be seen that the FPD and FPD50 oriented at 0° can be manufactured without support structures. Contrariwise, the LWD design solutions require support structures in all the investigated orientations. In particular, the GD is not self-supporting in spite of the design requirements imposed for optimisation. As a result, a significant amount of support material is needed for manufacturing. The weight of auxiliary material is higher for APF since the slicer the droplet-based deposition requires full-supporting structures. On the other hand, since FFF admits a certain level of bridging, less material is used for part supporting in this process.

All the other build orientations determine an increase of the auxiliary material. This result is expected due to the shape of the PSFS, the curvature of which does not allow for self-supporting. Therefore, the geometry of the specific part

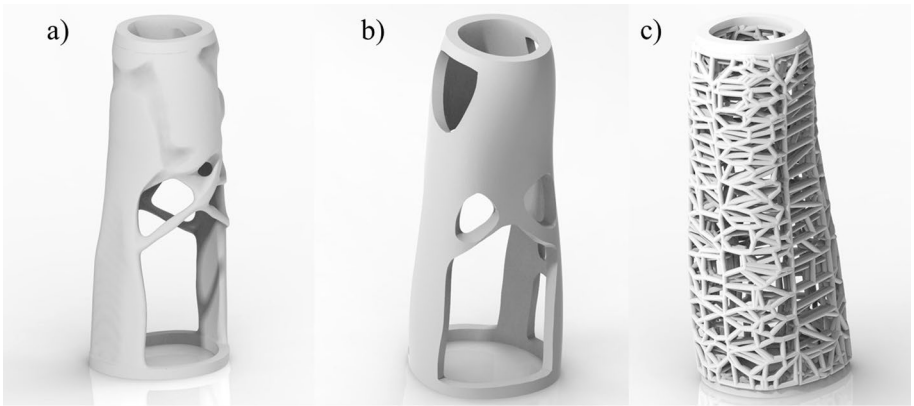

Fig. 4 Models obtained via **a** GD, **b** TO and **c** LS

Table 4 Results of slicing on APF

Design	α (°)	n_p	t_b (min)	t_{bp} (min)	m_p (g)	m_s (g)
FPD	0	1	184	184.00	11.49	0.00
FPD	45	1	330	330.00	11.37	28.40
FPD	90	1	260	260.00	11.28	22.74
FPD	0	30	5796	193.20	344.84	0.00
FPD	45	8	2652	331.50	90.97	223.33
FPD	90	8	2091	261.38	90.26	181.89
FPD50	0	1	130	130.00	6.98	0.00
FPD50	45	1	279	279.00	6.75	28.40
FPD50	90	1	213	213.00	6.48	22.74
FPD50	0	30	4183	139.43	209.26	0.00
FPD50	45	8	2250	281.25	53.97	223.33
FPD50	90	8	1718	214.75	51.83	181.89
GD	0	1	180	180.00	5.93	5.94
GD	45	1	304	304.00	5.89	35.90
GD	90	1	197	197.00	5.86	16.94
GD	0	20	3598	179.90	118.57	118.81
GD	45	8	2462	307.75	47.13	287.18
GD	90	8	1587	198.38	46.88	135.49
TO	0	1	182	182	4.45	2.52
TO	45	1	236	236	4.50	7.69
TO	90	1	156	156	4.53	5.69
TO	0	20	3638	181.9	89.08	50.47
TO	45	8	1885	235.63	36.00	61.55
TO	90	8	1250	156.25	36.20	45.48
LS	0	1	417	417.00	6.92	23.43
LS	45	1	529	529.00	6.93	62.95
LS	90	1	411	411.00	6.97	34.04
LS	0	20	8386	419.30	138.32	468.13
LS	45	8	4260	532.50	55.42	503.51
LS	90	8	3300	412.50	55.72	272.31

to be analysed must be closely investigated to determine the optimal build orientation.

As far as building time t_b is concerned, it is possible to notice that the APF process is significantly slower than FFF on all the investigated configurations. This result is consistent with the feed rates adopted for deposition, which have been shown in Table 1.

The building time shows that the FPD50 solution allows for a relevant reduction of the building time compared with FPD due to the lower number of lines used for infilling. GD and TO allow for reducing t_b since less material is deposited and, as a consequence, fewer movements are necessary. This effect is almost negligible for APF, while it becomes relevant in the case of FFF. On the other hand, LS determines an increase in t_b. Such a result can be explained if considering that this design requires more contours during printing compared to the original part. As the deposition speed used for contouring is considerably lower (see Tables 1 and 2), an increase in processing time is observed in both APF and FFF.

The 45° and 90° part orientations lead to higher values of t_b because of the need for depositing also the support material. Moreover, additional movements are necessary to move the second nozzle to the deposition zone and back.

3.3 Life cycle impact assessment

Figures 5 and 6 summarise the EndPoint (EP) indicators for APF and FFF, respectively. Specifically, EIs on Human Health (HH), Ecosystem Quality (EQ) and Resources Depletion (RD) are shown.

Comparing Figs. 5 and 6, it can be seen that the EIs of APF are considerably higher, especially as far as EQ and RD are concerned. This result is expected since the APF-2X 300K is an industrial machine whose architecture is considerably more complex than the Prusa i3 MK3S.

Table 5 Results of slicing on FFF

Design	α (°)	n_p	t_b (min)	t_{bp} (min)	m_p (g)	m_s (g)
FPD	0	1	112	112.0	11.73	0.00
FPD	45	1	166	166.0	11.46	6.91
FPD	90	1	142	142.0	11.07	4.93
FPD	0	48	5430	113.1	560.24	0.00
FPD	45	18	3000	166.7	205.21	124.64
FPD	90	18	2572	142.9	198.31	88.07
FPD50	0	1	90	90.0	8.74	0.00
FPD50	45	1	148	148.0	8.82	6.92
FPD50	90	1	130	130.0	9.43	4.89
FPD50	0	48	1460	30.4	416.68	0.00
FPD50	45	18	2664	148.0	157.72	124.64
FPD50	90	18	2347	130.4	168.67	88.07
GD	0	1	89	89.0	5.90	1.60
GD	45	1	134	134.0	5.85	6.98
GD	90	1	102	102.0	5.81	3.30
GD	0	48	4350	90.6	280.34	79.40
GD	45	18	2429	134.9	104.26	125.70
GD	90	18	1830	101.7	103.54	59.39
TO	0	1	78	78.0	5.51	3.48
TO	45	1	129	129.0	6.28	7.6
TO	90	1	90	90.0	6.41	3.81
TO	0	48	3767	78.5	259.12	166.85
TO	45	18	2346	130.3	111.23	136.85
TO	90	18	1624	90.2	113.57	68.63
LS	0	1	222	222.0	6.36	5.02
LS	45	1	280	280.0	6.24	11.71
LS	90	1	244	244.0	6.15	7.29
LS	0	42	9069	215.9	207.71	230.89
LS	45	18	4991	277.3	111.32	210.80
LS	90	18	4428	246.0	109.72	131.28

Figure 5 shows that the energy consumption of APF contributes significantly to EQ and HH EIs. On the other hand, these impacts are almost completely driven by the machine Life Cycle (LC) in the case of FFF. This can be explained if considering that the APF-2X 300K uses a heated building chamber. As discussed by [46], the build chamber heating is responsible for most of the energy demand of industrial-grade 3D printers.

As far as RD is concerned, it is evident that the APF impacts are deeply affected by the adoption of disposable building plates. This is in line with the findings of [37]. The impacts of consumables can be dramatically reduced by nesting multiple parts in the same build job. This effect can be seen in Fig. 7, which shows the RD impact for each combination of design and PBO.

By observing Fig. 7, it can be noticed that the PBO has a tremendous impact on the number of parts and, as a consequence, on RD. As far as 0° orientation is concerned, FPD and FPD50 result in more parts compared with GD , TO and LS. The reason is that the available printing space is reduced when two nozzles are used for printing, i.e. when support material is necessary.

Surprisingly, the contribution of material consumption to EIs is marginal. This is an interesting result since it allows concluding that the LWD itself is not sufficient to reduce the process EIs. Contrariwise, it is possible to notice that most indicators are governed by machine LC and energy consumption, which are both allocated on the basis of the printing time. As a result, the design solutions minimising printing time appear to be the most sustainable. Specifically, the minimum impacts of APF production are achieved by FPD50 oriented at 0°, while the FPD and GD are almost equivalent. The LS solution leads to the highest EIs. These findings are consistent with the values of t_b presented in Table 4.

In the case of FFF, the FPD50 and GD solutions are equally beneficial on HH and EQ. These solutions have almost the same building time (see Table 5). On the other

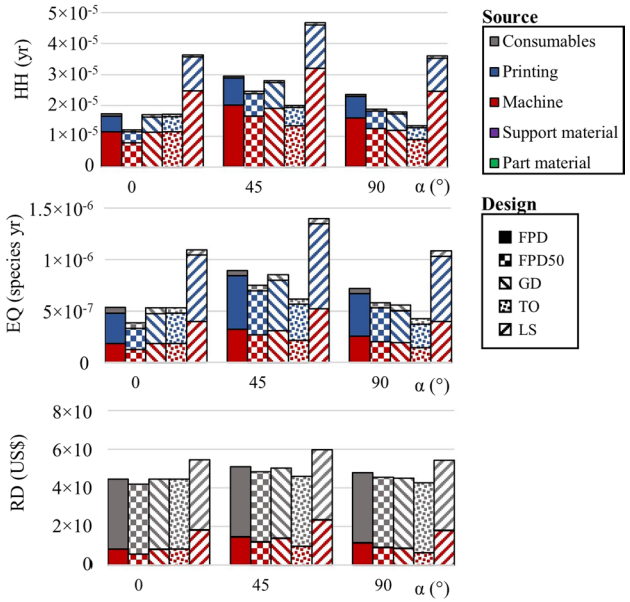

Fig. 5 EP LCIA of APF parts (one part per printing job)

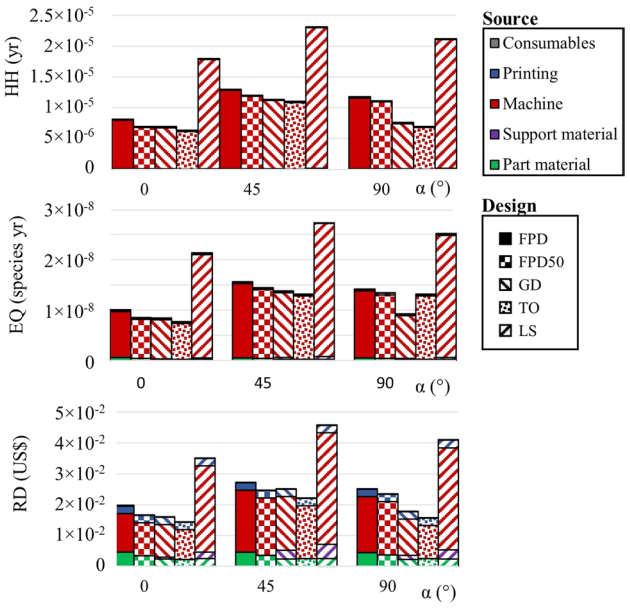

Fig. 6 EP LCIA of FFF parts (one part per printing job)

hand, the GD solution is slightly preferable as far as RD is concerned due to the lower material consumption. On the other hand, TO offers a significant saving on building time, as shown in Table 5. This in turn determines a benefit on all the EI indicators. This can be explained if considering the lower mass of support structures if compared with GD and the lower part mass compared with FPD50 (see Table 5).

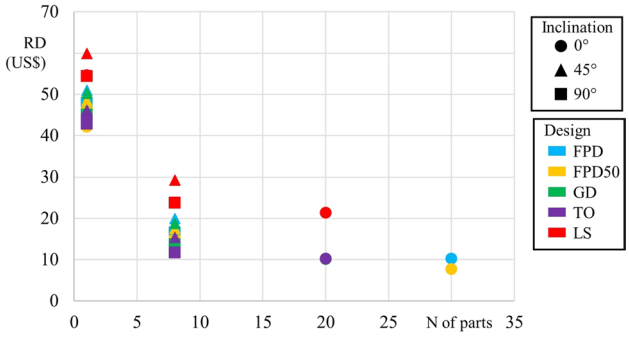

Fig. 7 RD impacts of APF with different number of parts in the same build job

In FFF, the impact of consumables is less pronounced due to the high number of prints which can be performed on a PolyEtherImide (PEI) building plate [42].

4 Extendability of the findings

It is important to mention that, since all the results presented in the previous sections have been calculated on the case study, the findings are limited to the specific combinations of product design and machine. Specifically, the geometry of the initial part and its application strongly affect the quantitative results of the LCA. Nonetheless, it is possible to draw some more general conclusions based on the parameters of the analysed building jobs. In particular, a pivotal role of building time has been observed. This can also be seen in Fig. 8, which shows the environmental impacts of products as a function of the building time per part.

It is possible to highlight that all the impacts increase almost linearly with the building time per part. Therefore, during the redesign of parts, close attention must be paid to the building time of the new part. This is due to the predominant role of energy consumption, in line with findings by [46].

It is worth mentioning that the considerations presented in this study are limited to the scope of MEX processes as those analysed in the case study. Indeed, the vast field of AM includes several technologies that profoundly differ one from the other [47]. For example, in Liquid Crystal Display (LCD) processes the building time and energy consumption are not affected by the complexity of shapes, nor by the number of parts per build job, but only by the number of layers [48]. Moreover, support structures are not necessary in the case of some technologies, e.g. polymer Powder Bed Fusion (PBF) [49]. Therefore, specific studies will be carried out in the future in order to investigate how LWD strategies affect the EIs of other AM processes.

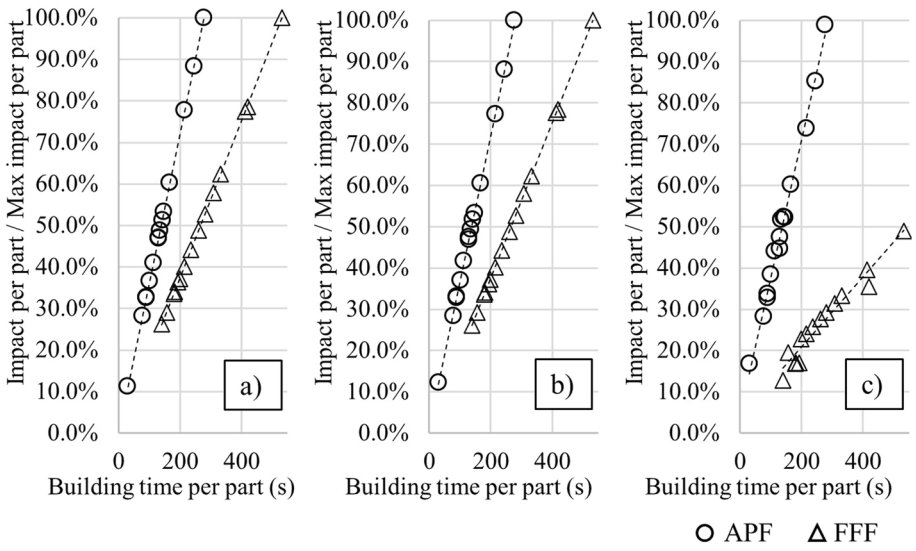

Fig. 8 EIs on **a** HH, **b** EQ and **c** RD as a function of the building time per part. EIs per part are reported as a percentage of the maximum observed value

5 Conclusions

This study gave an in-depth insight into the role of LWD on EIs of deposition-based AM production. The main result emerging from findings is that benefits derived from part weight reduction marginally contribute to the overall sustainability of the process. On the other hand, a leading role is played by the production time, which governs the impacts on HH and EQ. This means that the EIs of complicated LWD, such as LS, are higher than those of the original part in spite of material savings. GD appears more effective than LS in reducing EIs, especially in the case of FFF. However, this design strategy is highly time-consuming, which affects the efficiency of the design process. As a result, reducing the infill percentage of parts is found to be the more effective strategy to simultaneously reduce the part weight and EI.

As far as FFF is concerned, the best results are obtained by means of TO, which allows for a considerable reduction of the building time. In the case of APF, the EIs of TO are similar to those of GD. However, the computational cost of the former is significantly lower.

It is worth remarking that these findings are strictly connected to the geometry of the investigated case study. Nonetheless, a general dependency of EIs on the building time can be highlighted.

In the case of APF technology, a considerable impact is due to the use of disposable building plates. For this reason, nesting the maximum number of parts in the same build job is crucial to minimise the RD of the process.

Findings also highlight the pivotal role of PBO in EIs. In fact, this aspect deeply affects the building time, amount of support material and number of parts which can be nested on the building plate. PBO should be thus considered from the very first phases of LWD to effectively achieve environmental benefits. Future work will be thus dedicated to the integration of LCA methods into automated LWD techniques to allow for a sustainability-driven mass reduction in products for AM. This will require dedicated studies to explore the effects of LWD on the EIs of different AM processes and geometries.

Acknowledgements Authors would like to thank the MIUR (Italian Ministry of University and Research) for financing this study and PTC for supporting with software licences.

Funding Open access funding provided by Alma Mater Studiorum - Università di Bologna within the CRUI-CARE Agreement.

Data availability Raw data used in this study can be provided on request to the authors.

References

1. Dilberoglu UM, Gharehpapagh B, Yaman U, Dolen M (2017) The role of additive manufacturing in the era of industry 4.0. Proced Manuf 11:545–554. https://doi.org/10.1016/j.promfg.2017.07.148
2. Ngo TD, Kashani A, Imbalzano G, Nguyen KTQ, Hui D (2018) Additive manufacturing (3D printing): a review of materials, methods, applications and challenges. Compos Part B Eng 143:172–196. https://doi.org/10.1016/j.compositesb.2018.02.012

3. Grand View Research: 3D Printing Market Size, Share & Trends Analysis Report By Component, By Printer Type (Desktop, Industrial), By Technology, By Software, By Application, By Vertical, By Material, By Region, And Segment Forecasts, 2021 - 2028. Technical report (2021). https://www.grandviewresearch.com/industry-analysis/3d-printing-industry-analysis/methodology
4. 3D Hubs: 3D printing trends 2020 Industry highlights and market trend. Technical report (2020)
5. Garcia FL, Moris VAdS, Nunes AO, Silva DAL (2018) Environmental performance of additive manufacturing process - an overview. Rapid Prototyp J 24(7):1166–1177. https://doi.org/10.1108/RPJ-05-2017-0108
6. Kellens K, Mertens R, Paraskevas D, Dewulf W, Duflou JR (2017) Environmental impact of additive manufacturing processes: Does AM contribute to a more sustainable way of part manufacturing? Proced CIRP 61(Section 3):582–587. https://doi.org/10.1016/j.procir.2016.11.153
7. Khosravani MR, Reinicke T (2020) On the environmental impacts of 3D printing technology. Appl Mater Today 20:100689. https://doi.org/10.1016/j.apmt.2020.100689
8. Faludi J, Bayley C, Bhogal S, Iribarne M (2015) Comparing environmental impacts of additive manufacturing versus traditional machining via life-cycle assessment. Rapid Prototyp J 21(1):14–33. https://doi.org/10.1108/RPJ-07-2013-0067
9. Saade MRM, Yahia A, Amor B (2020) How has LCA been applied to 3D printing? A systematic literature review and recommendations for future studies. J Clean Prod 244:118803. https://doi.org/10.1016/j.jclepro.2019.118803
10. Faludi J, Baumers M, Maskery I, Hague R (2017) Environmental impacts of selective laser melting: Do printer, powder, or power dominate? J Ind Ecol 21:144–156. https://doi.org/10.1111/jiec.12528
11. Peng T, Kellens K, Tang R, Chen C, Chen G (2018) Sustainability of additive manufacturing: an overview on its energy demand and environmental impact. Addit Manuf 21(April):694–704. https://doi.org/10.1016/j.addma.2018.04.022
12. Thompson MK, Moroni G, Vaneker T, Fadel G, Campbell RI, Gibson I, Bernard A, Schulz J, Graf P, Ahuja B, Martina F (2016) Design for additive manufacturing: trends, opportunities, considerations, and constraints. CIRP Ann Manuf Technol 65(2):737–760. https://doi.org/10.1016/j.cirp.2016.05.004
13. Feng J, Fu J, Lin Z, Shang C, Li B (2018) A review of the design methods of complex topology structures for 3D printing. Vis Comput Ind Biomed Art 1(1):1–16. https://doi.org/10.1186/s42492-018-0004-3
14. Pan C, Han Y, Lu J (2020) Design and optimization of lattice structures: a review. Appl Sci 10:6374
15. Plocher J, Panesar A (2019) Review on design and structural optimisation in additive manufacturing: towards next-generation lightweight structures. Mater Des 183:108164. https://doi.org/10.1016/j.matdes.2019.108164
16. Krish S (2011) A practical generative design method. Comput Aided Des 43(1):88–100. https://doi.org/10.1016/j.cad.2010.09.009
17. Marsh A (2008) Generative and performative design: a challenging new role for modern architects **2008**(c)
18. Pollák M, Török J (2022) Use of generative design tools in the production of design products using 3D printing technology. TEM J 11(1):249–255
19. Taufek T, Adenan MS, Manurung YHP, Sulaiman SA, Zaid NS, Romzi NAS (2021) 3D metal printing using generative design and numerical computation. In: Osman Zahid MN, Abdul Sani AS, Mohamad Yasin MR, Ismail Z, Che Lah NA, Mohd Turan F (eds) Recent trends in manufacturing and materials towards industry 4.0. Springer, Singapore, pp 839–849
20. Daynes S, Feih S (2022) Bio-inspired lattice structure optimisation with strain trajectory aligned trusses. Mater Des 213:110320. https://doi.org/10.1016/j.matdes.2021.110320
21. Porter DA, Di MA, Badhe Y, Parikh AR (2022) Nylon lattice design parameter effects on additively manufactured structural performance. J Mech Beh Biomed Mater 125:104869. https://doi.org/10.1016/j.jmbbm.2021.104869
22. Böckin D, Tillman AM (2019) Environmental assessment of additive manufacturing in the automotive industry. J Clean Prod 226:977–987. https://doi.org/10.1016/j.jclepro.2019.04.086
23. Huang R, Riddle M, Graziano D, Warren J, Das S, Nimbalkar S, Cresko J, Masanet E (2016) Energy and emissions saving potential of additive manufacturing: the case of lightweight aircraft components. J Clean Prod 135:1559–1570. https://doi.org/10.1016/j.jclepro.2015.04.109
24. Mami F, Revéret JP, Fallaha S, Margni M (2017) Evaluating eco-efficiency of 3D printing in the aeronautic industry. J Ind Ecol 21:37–48. https://doi.org/10.1111/jiec.12693
25. Niaki MK, Torabi SA, Nonino F (2019) Why manufacturers adopt additive manufacturing technologies: the role of sustainability. J Clean Prod 222:381–392. https://doi.org/10.1016/j.jclepro.2019.03.019
26. Ribeiro I, Matos F, Jacinto C, Salman H, Cardeal G, Carvalho H, Godina R, Peças P (2020) Framework for life cycle sustainability assessment of additive manufacturing. Sustainability (Switzerland) 12(3):929. https://doi.org/10.3390/su12030929
27. Ford S, Despeisse M (2016) Additive manufacturing and sustainability: an exploratory study of the advantages and challenges. J Clean Prod 137:1573–1587. https://doi.org/10.1016/j.jclepro.2016.04.150
28. Tagliaferri V, Trovalusci F, Guarino S, Venettacci S (2019) Environmental and economic analysis of FDM, SLS and MJF additive manufacturing technologies. Materials 12(24):4161. https://doi.org/10.3390/ma12244161
29. Gebler M, Schoot Uiterkamp AJM, Visser C (2014) A global sustainability perspective on 3D printing technologies. Energy Policy 74(C):158–167. https://doi.org/10.1016/j.enpol.2014.08.033
30. Fruggiero F, Lambiase A, Bonito R, Fera M (2019) The load of sustainability for Additive Manufacturing processes. Proced Manuf 41:375–382. https://doi.org/10.1016/j.promfg.2019.09.022
31. Le VT, Paris H (2018) A life cycle assessment-based approach for evaluating the influence of total build height and batch size on the environmental performance of electron beam melting. Int J Adv Manuf Technol 98(1–4):275–288. https://doi.org/10.1007/s00170-018-2264-7
32. Mele M, Campana G (2020) Sustainability-Driven Multi-Objective Evolutionary Orienting in Additive Manufacturing. Sustain Product Consumpt 23:138–147. https://doi.org/10.1016/j.spc.2020.05.004
33. Bourhis FL, Kerbrat O, Dembinski L, Hascoet JY, Mognol P (2014) Predictive model for environmental assessment in additive manufacturing process. Procedia CIRP 15:26–31. https://doi.org/10.1016/j.procir.2014.06.031
34. Ma J, Harstvedt JD, Dunaway D, Bian L, Jaradat R (2018) An exploratory investigation of additively manufactured product life cycle sustainability assessment. J Clean Prod 192:55–70. https://doi.org/10.1016/j.jclepro.2018.04.249
35. Yi L, Glatt M, Sridhar P, de Payrebrune K, Linke BS, Ravani B, Aurich JC (2020) An eco-design for additive manufacturing framework based on energy performance assessment. Addit Manuf 33:101120. https://doi.org/10.1016/j.addma.2020.101120
36. Al-Ghamdi KA (2019) Sustainable FDM additive manufacturing of ABS components with emphasis on energy minimized and time efficient lightweight construction. Int J Lightweight Mater Manuf 2(4):338–345. https://doi.org/10.1016/j.ijlmm.2019.05.004

37. Mele M, Campana G, Fumelli G (2021) Environmental impact assessment of Arburg plastic freeforming additive manufacturing. Sustain Product Consumpt 28:405–418. https://doi.org/10.1016/j.spc.2021.06.012
38. Welsh NR, Malcolm RK, Devlin B, Boyd P (2019) Dapivirine-releasing vaginal rings produced by plastic freeforming additive manufacturing. Int J Pharm 572(July):118725. https://doi.org/10.1016/j.ijpharm.2019.118725
39. Emzain ZF, Amrullah US, Mufarrih A, Qosim N (2021) Design optimization of sleeve finger splint model using Finite Element. Analysis 19:147–152
40. Zolfagharian A, Gregory TM, Bodaghi M, Gharaie S, Fay P (2020) Patient-specific 3D-printed splint for mallet finger injury. Int J Bioprint 6(2):1–13. https://doi.org/10.18063/ijb.v6i2.259
41. Hentschel L, Kynast F, Petersmann S, Holzer C, Gonzalez-Gutierrez J (2020) Processing conditions of a medical grade poly(Methyl methacrylate) with the arburg plastic freeforming additive manufacturing process. Polymers 12(11):1–15. https://doi.org/10.3390/polym12112677
42. Campana G, Mele M, Ciotti M, Rocchi A (2021) Environmental impacts of self-replicating three-dimensional printers. Sustain Mater Technol 30(May):00335. https://doi.org/10.1016/j.susmat.2021.e00335
43. Wernet G, Bauer C, Steubing B, Reinhard J, Moreno-Ruiz E, Weidema B (2016) The ecoinvent database version 3 (part I): overview and methodology. Int J Life Cycle Assess 21(9):1218–1230. https://doi.org/10.1007/s11367-016-1087-8
44. Huijbregts MAJ, Steinmann ZJN, Elshout PMF, Stam G, Verones F, Vieira M, Zijp M, Hollander A, van Zelm R (2017) ReCiPe2016: a harmonised life cycle impact assessment method at midpoint and endpoint level. Int J Life Cycle Assess 22(2):138–147. https://doi.org/10.1007/s11367-016-1246-y
45. Manfredi S, Allacker K, Pelletier N, Chomkhamsri K, de Souza DM (2012) Product environmental footprint (PEF) guide
46. Bernardez LD, Campana G, Mele M, Sanguineti J, Sandre C (2022) Effects of infill patterns on part performances and energy consumption in acrylonitrile butadiene styrene fused filament fabrication via industrial - grade machine. Progr Addit Manuf 8(2):117–129. https://doi.org/10.1007/s40964-022-00316-4
47. Gibson I, Rosen D, Stucker B, Khorasani M (2021) Additive manufacturing technologies. Springer, Boston, pp 1–459
48. Mele M, Campana G (2022) Advancing towards sustainability in liquid crystal display 3D printing via adaptive slicing. Sustain Product Consumpt 30:488–505. https://doi.org/10.1016/j.spc.2021.12.024
49. Wang Y, Xu Z, Wu D, Bai J (2020) Current status and prospects of polymer powder 3D printing technologies. Materials 13(10):2406. https://doi.org/10.3390/ma13102406